ELSEVIER

Journal of Structural Geology 27 (2005) 1750–1764

JOURNAL OF STRUCTURAL GEOLOGY

www.elsevier.com/locate/jsg

Deformation regime variations in an arcuate transpressional orogen (Ribeira belt, SE Brazil) imaged by anisotropy of magnetic susceptibility in granulites

Marcos Egydio-Silva[a,*], Alain Vauchez[b], Maria Irene B. Raposo[a], Jérôme Bascou[c], Alexandre Uhlein[d]

[a]*Instituto de Geociências, Universidade de Sao Paulo, Sao Paulo, Brazil*
[b]*Laboratoire de Tectonophysique, Université de Montpellier II CNRS, Montpellier, France*
[c]*Laboratoire de Transferts Lithosphériques, Université de Saint Etienne, Saint Etienne, France*
[d]*Instituto de Geociências, Universidade Federal de Minas Gerais, Minas Gerais, Brazil*

Received 23 September 2004; received in revised form 24 May 2005; accepted 2 June 2005
Available online 10 August 2005

Abstract

The Ribeira belt of southeastern Brazil displays an arcuate shape, with a structural trend that varies from ~NS in the northern domain to ENE–WSW in the southern domain. This curvature is accompanied by a transition from contraction-dominated to transcurrent-dominated tectonics. The transition in deformation regime is accommodated in the central domain of the belt where granulitic rocks dominate and mineral-stretching lineations are commonly concealed by metamorphic recrystallization. We present anisotropy of magnetic susceptibility (AMS) data from 664 samples from 62 sites in high-temperature gneisses, granulites and migmatites of the transitional, central domain of the belt, with the aim of investigating: (1) how well AMS allows one to map the mineral-stretching lineation and foliations in domains displaying a complex kinematic framework and (2) to investigate the kinematic pattern at the transition between the thrusting dominated and a wrench-faulting dominated orogenic segments.

The mean magnetic susceptibility is 7.54×10^{-3} SI. The degree of anisotropy varies from 1.32 up to 4.31, with an average value of 1.53. The shape parameter T is generally >0 meaning that the AMS ellipsoid is dominantly oblate. Magnetic lineations and foliations form a consistent pattern correlated with the modification of the structural characteristics observed along the Ribeira belt. In the southern wrench-fault-dominated domain, the magnetic lineation is subhorizontal, parallel to the trend of the steeply dipping magnetic foliation. This correlation with the fabric observed in mylonites suggests that the magnetic fabric is a valid proxy of the tectonic fabric in granulites. Results from the northern domain show that it comprises two sub-domains both displaying a ~NS-trending magnetic foliation. Eastward, over a broad area, the magnetic foliation is consistently steeply dipping and bears a shallowly to moderately plunging magnetic lineation. Westward, the dip of the foliation decreases progressively and the lineation rotates from nearly parallel to nearly orthogonal to the trend of the foliation, suggesting a progressive transition from transcurrent to contractional tectonics. At the junction between the northern and southern domains, the magnetic fabric is composite: the magnetic foliation displays a constant NNE–SSW orientation, but the magnetic lineation spreads within the foliation plane from parallel to normal to the foliation direction. The AMS pattern mapped in the Central Ribeira belt supports a scenario in which the transcurrent and contractional deformation regimes are coeval, with a transition between the two regimes accommodated progressively over a large transpressional area where both strain regimes were active.

Keywords: Ribeira belt; Magnetic fabrics; Strain partition; Transpressional deformation; Anisotropy of magnetic susceptibility

1. Introduction

Understanding large-scale deformation in orogenic domains that have undergone complex deformation regimes, i.e. transpression or transtension, is not straightforward, given the lack of a simple relationship between the structural fabric and the deformation field (Lin and Jiang,

* Corresponding author. Tel.: +55 11 3091 3912; fax: +55 11 3091 4258.
E-mail address: megydios@usp.br (M. Egydio-Silva).

0191-8141/$ - see front matter © 2005 Elsevier Ltd. All rights reserved.
doi:10.1016/j.jsg.2005.06.001

2001). These authors argue that, in order to constrain the deformation in a curved, transpressional shear zone, a detailed kinematic analysis of differently oriented segments is needed. Moreover, because of the strain partitioning that commonly occurs in such curved domains, a good knowledge of the kinematic pattern at the scale of the tectonic system is required to understand how complex deformation regimes were accommodated. The importance of mapping foliation and stretching lineation is widely recognized in modern tectonic studies since these structures represent the most basic and fundamental observations directly related to the flow of rocks in orogenic areas. Consequently, the absence of macroscopically visible planar and/or linear structures impedes any reliable kinematic analysis, a situation that commonly arises in high-grade metamorphic terrains. Kinematic analysis in granulitic and anatectic domains is made difficult or even impossible since the intense recrystallization and partial melting of the rocks hinder a systematic measurement of the tectonic fabric, especially the lineation. However, granulites and migmatites usually predominate in the internal domains of ancient orogens. These rocks have recorded the processes active in the deep crust, and are therefore of primary importance to understanding large-scale deformation in the crustal roots of orogens. Therefore, the absence of kinematic data from these domains significantly hinders the development of relevant geodynamic models.

This difficulty arises in the Neoproterozoic Ribeira belt, southeast Brazil (Fig. 1), which is characterized by a change in its structural trend from ~NS in the northern domain, to ENE–WSW southward. This curvature is correlated with a transition from thrusting dominated deformation to wrench-faulting dominated transpression. How strain is accommodated in the transition domain is still poorly understood, especially because of the scarcity of visible mineral-stretching lineations in the granulites and granulitic migmatites that are the dominant lithologies of the area.

To overcome these problems, the anisotropy of magnetic susceptibility (AMS) technique provides a powerful approach allowing one to indirectly unravel mineral preferred orientation fabrics (e.g. Hrouda, 1982, 1993; Borradaile, 1988, 1990, 2001; Bouchez et al., 1990; Rochette et al., 1992; Borradaile and Henry, 1997; Bouchez, 1997; Ferré et al., 2003). The AMS technique was initially applied to investigate the primary fabric in sedimentary rocks (e.g. Ellwood, 1980; Flood et al., 1985) and to determine the fabric associated with magmatic flow in igneous rocks (e.g. Ellwood, 1982; Knight et al., 1986; Bouchez, 2000). More recently it was shown that AMS may be useful in a larger variety of rocks, encompassing granulites, peridotites and migmatites (Borradaile and Lagroix, 2000, 2001; Bascou et al., 2002; Borradaile and Gauthier, 2003; Ferré et al., 2003). The principal axes of susceptibility are usually close to the strain axes, indicating that the magnetic fabric is a strain-induced phenomenon, and suggesting that magnetic fabric measurements are at least qualitatively significant with respect to the strain history of rocks (e.g. Goldstein and Brown, 1988).

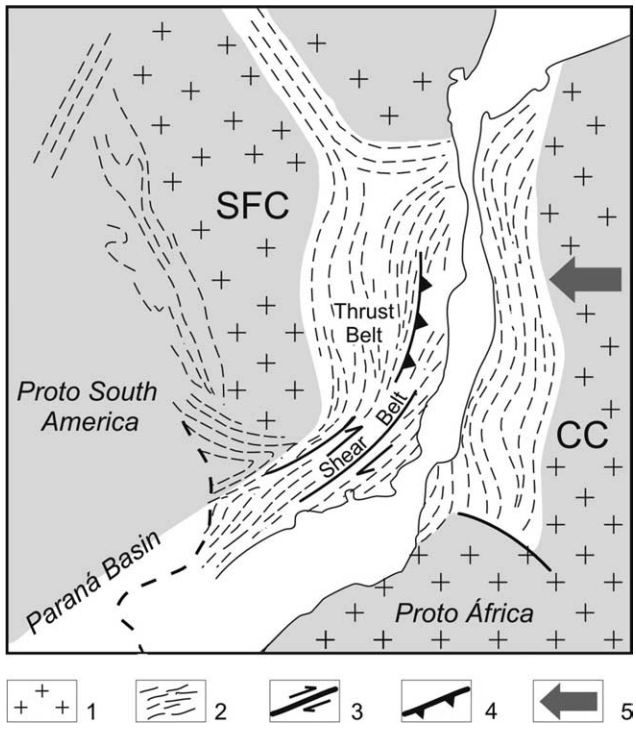

Fig. 1. Sketch map of the Ribeira/Araçuaí belt showing the curved shape and the compressive and transpressive character of the northern and southern domains, respectively. (1) Cratonic areas (SFC, São Francisco craton; CC, Congo craton). (2) Ribeira/Araçuaí fold belt (Thrust and Shear belt). (3) Transcurrent faults. (4) Thrust faults. (5) Large-scale continent–continent convergence responsible for the Neoproterozoic orogeny.

We performed AMS measurements in granulites and migmatitic gneisses from the Ribeira belt, with a twofold purpose: (1) to verify how well this technique allows one to map the mineral-stretching lineation in domains displaying a complex kinematic framework, and (2) to more precisely define the kinematic pattern at the transition between the thrusting-dominated and the wrench-faulting-dominated domains of the Ribeira belt. A detailed image of the kinematic field in such a transitional domain is essential to understand: (1) whether orogen-normal thrusting and orogen-parallel transcurrent motions were coeval or not, and (2) how changes in dominant deformation regime are accommodated at the regional scale.

2. Geological setting

The Neoproterozoic Ribeira belt extends over more than 1500 km along the southeastern coast of Brazil (Fig. 1). The northern and central parts of the belt border the eastern and the southeastern margins of the São Francisco craton. Southward, the Ribeira belt intersects the Neoproterozoic Brasilia belt. Its southern termination is hidden beneath the Paraná basin. This orogen developed in response to the

convergence between the São Francisco and the Congo cratons during the Neoproterozoic Brasiliano orogeny (~600 Ma). This belt displays unusual structural characteristics suggesting that the southern termination of the São Francisco craton profoundly influenced the mechanical response of the lithosphere during the continental collision. At ~21°S latitude, the structural trend changes orientation from NS to NNE within the northern part of the belt to ENE in the southern part. This curvature is spatially correlated to the southern termination of the São Francisco craton. The change in structural trend is associated with a major variation in tectonic style along the belt. The northern Ribeira belt is dominated by thrusting towards the craton, whereas strike slip faulting and transpressive tectonics dominate southward (Fig. 1). Vauchez et al. (1994) used finite element modelling to demonstrate that the variation in tectonic style along the Ribeira belt may be due to the lithosphere-scale rheological heterogeneity induced by the termination of the cold and stiff São Francisco craton.

In this study, we focus on the structure of the central part of the belt, where the transition from contractional to transcurrent tectonics is accommodated. For simplicity sake, the studied area has been subdivided into three distinct domains according to the predominant tectonic regime (Fig. 2). The northern domain is characterized by low-angle foliation, the southern domain by vertical foliations and orogen-parallel strike-slip shear-zones, and the central domain makes the junction between the other two domains and thus displays composite characteristics. The lithology is dominated by sequences of middle to lower crustal rocks, especially granulites and migmatitic gneisses, which protoliths have been dated at 2220±27 Ma (U/Pb ages; Sollner et al., 1991). These rocks have subsequently undergone tectonic, magmatic and metamorphic processes during the Neoproterozoic Brasiliano orogeny.

The southern domain is made up of an assemblage of high temperature (granulite to upper amphibolite facies) gneisses and mylonites, involving granulites of noritic to granodioritic composition, garnet–biotite–plagioclase gneisses, amphibolites, and some biotite-rich migmatites, generally with coarse-grained porphyroclastic microstructure (Egydio-Silva et al., 2002; Fig. 3). The granulites are composed of quartz, plagioclases ($An_{20–40}$), orthopyroxene, garnets (almandine/grossular rich), ±K-feldspars, ±clinopyroxene, ±hornblende. Biotite is abundant in the lower grade rocks, with muscovite totally absent. Minerals from the titanohematite solid solution and magnetite are usually present. Rock-forming minerals are segregated into elongated, nearly monomineralic layers or ribbons that mark the steeply dipping foliation (Fig. 4). The ribbons wrap around porphyroclasts of plagioclase, garnet, orthopyroxene and/or clinopyroxene. Preferred orientation of orthopyroxene, amphibole and feldspar also marks the foliation. At the grain scale, the mylonites display microstructures (recovery, grain boundary migration and extensive grain growth) indicating high temperature conditions prevailing during and after mylonitic deformation (Egydio-Silva et al., 2002).

The northern domain is essentially made up of granulite facies rocks (Fig. 3). They are orthogneisses, usually migmatitic, derived from norites, tonalites, granodiorites and alkali-charnockites. Ferromagnesian minerals in these granulites are predominantly hypersthene and hornblende. Subsidiary paragneisses containing biotite, quartz, plagioclase, garnet (almandine) and prismatic sillimanite are also present. A well-developed compositional layering parallel to the foliation is usually observed; it trends predominantly N10–30E and dips gently, and more locally steeply, eastward. Leucocratic veins of trondhjemitic to tonalitic composition are intruded along the layering/foliation. Stretching lineations are scarce; where observed lineations trend at a high angle to the foliation strike suggesting orogen-normal displacements. Kinematic indicators (Fig. 5) were observed by various authors (Trompette, 1994; Uhlein et al., 1998). In most cases, the flow direction cannot be reliably determined since no mineral-stretching lineation is observed. However, by assuming a stretching direction close to E–W, as observed from lineations at several localities, the kinematic indicators observed on EW-oriented surfaces consistently agree with westward thrusting (Fig. 5).

The central domain displays HT-tectonites similar to those that occur in the northern and southern domains. The internal geometry of this domain is characterized by coexistence of low-angle foliations and orogen-parallel, steeply dipping transcurrent shear zones. The metamorphic conditions that prevailed during thrusting- and wrench-faulting are similar ($T>750$ °C and $P=0.6–0.7$ GPa; Bascou et al., 2002) suggesting that the two deformation regimes were almost coeval (Egydio-Silva et al., 2002). Transcurrent shear zones several hundreds of metres thick display intense deformation accommodated under granulitic conditions (Fig. 3). Stretching lineations are usually observed within the transcurrent shear zones where they tend to be sub-horizontal. In domains characterized by shallowly dipping foliations, stretching lineations are rarely observed. However, when observed they trend normal to the belt.

3. Anisotropy of magnetic susceptibility (AMS)

The magnetic susceptibility (k) is an intrinsic physical property of materials, and may be regarded as their *magnetizability* (Butler, 1992). Rocks in which the intensity of magnetization (whether induced or remanent) depends on the direction of the applied magnetic field display *magnetic anisotropy*. The anisotropy of magnetic susceptibility (AMS) can be represented by a symmetrical second rank tensor (k_{ij}) that relates the intensity of the applied external field (H) to the acquired magnetization (M):

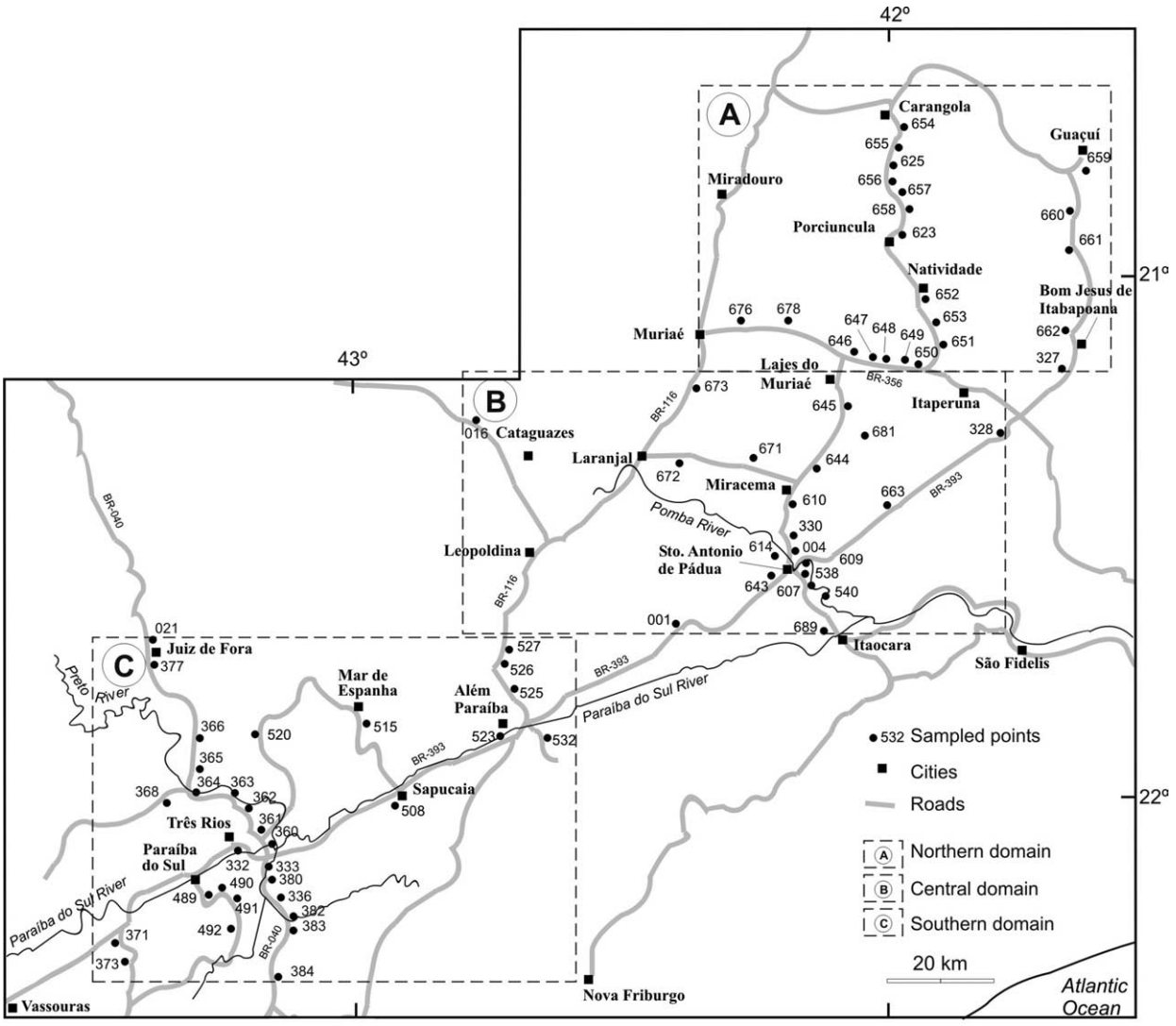

Fig. 2. Location of the 62 localities sampled for the AMS study.

$$M_i = K_{ij}H_j \quad (1)$$

In polyphase rocks, the mean susceptibility K_m is the sum of individual contributions of each dia-, para- and ferromagnetic mineral with respect to its volume contents (e.g. Siegesmund, 1996). For diamagnetic and paramagnetic minerals, the anisotropy of susceptibility is controlled by the crystallographic orientations of the mineral grains and is not significantly influenced by grain shape. However, for ferromagnetic minerals, among which magnetite and hematite are the most important, the grain shape largely influences the magnetic fabric (Borradaile, 1988).

In low magnetic fields ($\approx$0.1 mT), K is geometrically represented by a triaxial ellipsoid with axes $K_1 \geq K_2 \geq K_3$ (Hrouda, 1982; Borradaile, 1988). In general, K_1, the maximum susceptibility direction, is regarded as a proxy of the mineral lineation, and K_3, the minimum susceptibility direction, is close to the pole to the mineral foliation (plane containing K_1 and K_2). Bascou et al. (2002) have shown that a clear correlation exists between the AMS axes and the crystallographic preferred orientation of titanohematite and pyroxenes in granulite samples from the central Ribeira belt. This result supports AMS axes being used in granulites as proxies of the principal structural/kinematic axes, circumventing the difficulty in observing mesoscopic lineations and foliations.

3.1. Procedures, sampling and magnetic measurements

A total of 62 sites spanning from the northern to the southern domains of the Central Ribeira belt have been sampled. At each site, between 4 and 7 samples have been collected using a portable motor drill, and carefully oriented using both magnetic and solar compasses. Each sampled cylinder was cut into at least two specimens with a diameter of 2.5 cm and a height of 2.2 cm. As a result, the AMS was measured for a total of 664 specimens from all 62 sampled sites using a Kappabridge instrument (KLY-3S, Agico,

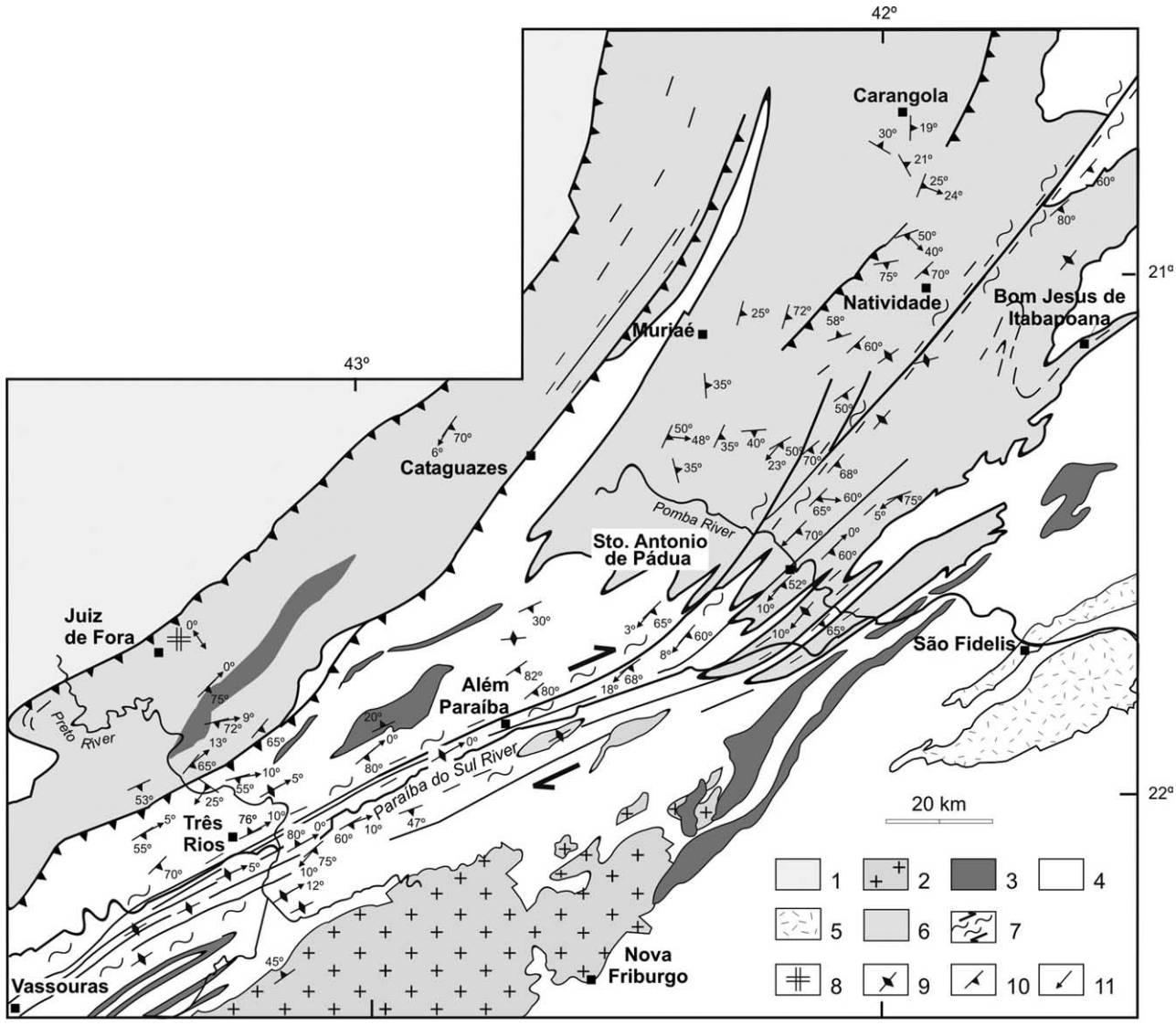

Fig. 3. Simplified geologic map of the central Ribeira/Araçuaí belt. (1) Polycyclic basement; (2) syntectonic granites; (3) quartzites and marbles (Italva group); charnockites; (4) gneisses and migmatites (Paraíba do Sul complex); (5) kinzigites-gneisses (Paraíba do Sul complex); (6) granulites and charnockites (Juiz de Fora complex); (7) mylonitic rocks; (8) horizontal foliation; (9) vertical foliation; (10) foliation; (11) lineation.

Czech Republic) and computed using the *Aniso software* (Jelinek, 1977).

3.2. Magnetic mineralogy and rock magnetism

The magnetic minerals responsible for the magnetic anisotropy in the studied sites were determined using several rock–magnetic experiments: (a) thermomagnetic curve determinations, (b) coercivity spectra from both anhysteretic remanence and alternating field (AF) demagnetization, (c) thermal demagnetization, (d) isothermal remanent magnetization (IRM) acquisition, and (e) hysteresis measurements (Raposo and Egydio-Silva, 2001).

The results suggest a mixture of magnetic minerals with a predominance of magnetite and titanohematite (hematite–ilmenite solid solution) and, in some samples, a minor quantity of sulphides such as pyrrhotite, which is revealed by the thermomagnetic curves (Raposo and Egydio-Silva, 2001). Since both para- and ferromagnetic minerals are present, the AMS is likely due to a combination of the preferred crystallographic orientations of titanohematite and paramagnetic matrix minerals, and to the shape anisotropy of magnetite grains (Bascou et al., 2002).

The AMS data are presented in Table 1 and Fig. 6. The mean magnetic susceptibility, expressed by $K_m=(K_1+K_2+K_3)/3$ in SI units, ranges from ~ 0.2 to $\sim 90\times 10^{-3}$ SI. This large variability is the result of the presence of a large variety of rocks in our set of samples (Hunt et al., 1995), involving amphibolite facies gneisses, granulites and charnockitic plutonic rocks. However, for most samples K_m is $<5\times 10^{-3}$ SI. The intensity of the anisotropy, or anisotropy degree, expressed by $P=K_1/K_3$, is relatively

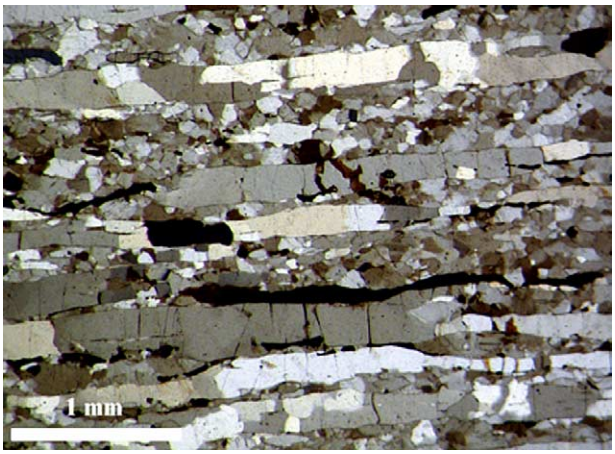

Fig. 4. Photomicrograph showing typical elongated titanohematite grain and polycrystalline quartz ribbons in granulite-facies mylonites from the Alem-Paraiba shear zone (southern domain) (crossed nicols).

Fig. 5. Asymmetric amphibolite boudins in HT-mylonites from the northern domain. A leucocratic melt was injected along the compositional layering and within the boudins. Assuming a lineation close to EW sub-horizontal, the asymmetry would suggest a top to west sense of shear. No reliable lineation was, however, observed at this outcrop (scale bar 5 cm).

high, as would be expected for metamorphic rocks, and spans from 1.03 up to 4.31; few samples, however, have $P>2$, resulting in an average value of ~1.53. The symmetry of the anisotropy ellipsoid is described by the Jelinek's parameter T ($T=(\ln F-\ln L)/(\ln F+\ln L)$ where $F=K_2/K_3$ and $L=K_1/K_2$). The value of T is 0 for a plane anisotropy ellipsoid, >0 for a uniaxial oblate ellipsoid and <0 for a uniaxial prolate ellipsoid. Systematic measurements show that most magnetic ellipsoids are oblate ($T>0$; Fig. 6). There is no clear correlation between P and T (Raposo and Egydio-Silva, 2001).

3.3. The AMS fabrics

3.3.1. The southern domain

A total of 28 sites were sampled with AMS measurements performed on 141 cylindrical specimens (Table 1). The magnetic susceptibility K_m is generally $<1.0\times10^{-3}$ SI (64.3%; Table 1 and Fig. 6a). The relatively low values of magnetic susceptibility for granulites (Hunt et al., 1995) reflect the felsic composition of most granulites from this area. Only a few sites display a significantly higher K_m corresponding to more basic compositions (e.g. K_m reaches 90.25 and 42.52×10^{-3} SI for sites RB365 and RB491, respectively). The degree of anisotropy P varies from 1.08 up to 2.95, with an average value of 1.64. The shape parameter T varies from −0.65 up to 0.89 with a mean value of 0.40. The magnetic ellipsoid is oblate for 68% of the sites, prolate for 18% and almost planar (although with $T>0$) for 14% of the sites.

The eigenvectors (K_1, K_2 and K_3) within the southern domain are well grouped (Fig. 7b). The K_3 directions lie close to the poles to the observed mylonitic foliation and the magnetic lineation (that is, the main concentration of K_1 directions) is clearly defined and parallel to the stretching lineation observed in the field. The mean orientations of K_1 and K_3 are, respectively, 19° to N51°E and 2° to N320°E, this latter value corresponding to a sub-vertical foliation plane oriented N50°E. The good qualitative agreement between the AMS axes and the field structural data (Fig. 3) is attributed to the high strain undergone by the mylonitic rocks, which resulted in a well-developed stretching lineation, foliation, and preferred crystallographic orientation of titanohematite and paramagnetic matrix minerals (Fig. 4; Bascou et al., 2002).

The map view of the magnetic foliation and lineation (domain C on Fig. 10) averaged at each site shows a consistent pattern over the entire area. Most magnetic foliations and lineations parallel the trend of the belt, even outside the main transcurrent shear zones observed in this area. This suggests that transcurrent motion parallel to the belt is largely distributed, even if strain localization occurs in mylonitic zones. Northwestward and southeastward of the dominantly transcurrent domain, several localities display a magnetic fabric more compatible with thrusting. This is coherent with a transpressional collision during which partitioned orogen-normal and orogen-parallel displacements may occur either concomitantly or successively (Lin and Jiang, 2001).

3.3.2. The northern domain

The measurements of AMS focussed on the granulitic rocks belonging to the Juiz de Fora complex, where the stretching lineation is only occasionally observed. We have sampled 19 sites and AMS individual measurements have been performed on 277 cylindrical specimens (Table 1).

The magnetic susceptibility ranges from ~0.25 to $\sim39\times10^{-3}$ SI. Twenty-six percent of the samples have $K_m>9\times10^{-3}$ SI; this denotes a larger heterogeneity of the magnetic mineralogy in the northern than in the southern domain (Raposo and Egydio-Silva, 2001). The degree of anisotropy P varies from 1.06 up to 2.04, with an average

Table 1

SITE	N/n	K_m (10^{-3})	Mean AMS parameters				Mean eigenvectors			
			L	F	P	T	K_{max}		K_{min}	
							Dec/inc	z/e	Dec/inc	z/e
Northern domain										
RB623	16/12	9.380	1.176	1.459	1.720	0.431	102/34	2/8	310/53	3/6
RB625	21/20	0.330	1.108	1.082	1.197	−0.110	91/11	3/5	209/68	3/9
RB646	30/28	25.193	1.108	1.079	1.204	−0.195	59/17	4/8	272/70	5/20
RB647	17/12	32.448	1.084	1.456	1.581	0.537	89/46	5/7	297/40	4/6
RB648	27/27	12.275	1.184	1.513	1.800	0.420	67/18	2/3	304/59	1/2
RB649	12/9	1.014	1.052	1.112	1.173	0.418	39/23	7/40	130/1	7/11
RB650	20/18	3.476	1.111	1.214	1.358	0.042	55/31	3/7	312/20	3/7
RB651	19/15	0.716	1.036	1.186	1.229	0.637	36/15	3/11	299/23	3/3
RB652	24/24	0.814	1.106	1.196	1.325	0.160	79/46	3/6	299/36	3/7
RB653	17/15	1.065	1.035	1.218	1.270	0.741	217/28	4/15	310/6	2/6
RB654	9/7	0.249	1.019	1.058	1.077	0.509	83/24	4/24	224/61	3/5
RB655	16/15	1.210	1.101	1.094	1.207	−0.079	67/60	5/10	205/24	6/14
RB656	22/20	0.813	1.044	1.052	1.098	0.066	18/77	3/7	218/12	4/6
RB657	10/9	0.988	1.051	1.065	1.119	0.115	65/57	6/13	260/32	6/8
RB658	13/13	0.640	1.022	1.032	1.055	0.126	38/37	7/9	245/50	4/15
RB659	16/10	6.820	1.112	1.094	1.215	−0.026	125/35	5/9	217/3	5/14
RB660	9/9	5.479	1.334	1.508	2.033	0.084	353/47	18/35	260/3	25/59
RB661	9/9	39.177	1.152	1.521	1.758	0.521	39/31	3/11	292/27	3/4
RB662	5/5	4.871	1.169	1.221	1.424	0.114	43/31	5/10	310/5	5/10
Central domain										
RB1	23/22	1.259	1.054	1.306	1.378	0.676	224/16	2/7	322/25	1/2
RB4	4/4	3.010	1.145	1.669	1.914	0.563	67/49	2/11	316/16	1/4
RB16	4/4	15.357	1.231	1.622	1.997	0.399	210/3	1/4	302/27	1/3
RB330	8/8	1.019	1.038	1.526	1.582	0.829	231/6	6/14	141/2	4/28
RB538	21/21	25.297	1.293	3.151	4.312	0.535	217/7	1/2	311/27	1/1
RB540	11/11	10.702	1.174	1.325	1.557	0.270	36/9	2/3	305/4	2/4
RB607	14/12	3.458	1.118	1.342	1.510	0.450	224/8	2/6	319/31	2/2
RB609	14/14	14.522	1.156	1.342	1.551	0.332	222/4	1/4	314/26	2/3
RB610	15/14	0.403	1.058	1.098	1.161	0.350	71/56	3/11	313/18	4/9
RB614	11/11	3.182	1.058	1.711	1.810	0.811	151/52	1/11	317/37	1/2
RB643	18/18	19.027	1.332	1.491	2.007	0.155	224/4	2/3	317/34	2/3
RB644	11/11	0.570	1.037	1.109	1.151	0.450	70/51	2/7	312/21	2/4
RB645	17/15	0.751	1.030	1.176	1.213	0.692	164/45	2/21	299/35	2/4
RB663	6/6	29.832	1.201	1.844	2.227	0.557	60/26	4/5	327/6	3/10
RB689	12/12	0.463	1.015	1.017	1.032	0.069	17/24	3/7	216/64	4/23
Southern domain										
RB21	4/4	1.211	1.359	1.388	1.886	0.034	81/7	1/2	301/81	1/1
RB332	21/17	0.221	1.021	1.133	1.158	0.735	58/35	3/5	148/0	3/5
RB336	4/4	0.577	1.161	1.243	1.450	0.095	273/52	14/19	174/7	14/20
RB360	4/4	0.653	1.106	1.241	1.374	0.358	183/3	1/8	91/37	2/6
RB361	4/4	0.215	1.022	1.169	1.195	0.751	128/33	1/9	38/1	1/1
RB362	4/4	8.132	1.521	1.115	1.693	−0.594	75/2	2/22	176/80	5/35
RB363	8/8	0.269	1.077	1.091	1.175	0.035	72/13	2/9	332/39	3/5
RB364	8/8	0.157	1.100	1.140	1.254	0.232	42/7	2/5	244/82	2/15
RB365	4/4	90.249	1.495	1.970	2.949	0.257	54/16	1/4	305/47	1/3
RB366	4/4	0.690	1.009	1.175	1.186	0.892	192/75	1/90	346/13	½
RB368	4/4	0.220	1.027	1.185	1.217	0.719	88/18	2/19	351/20	2/7
RB371	4/4	0.341	1.046	1.112	1.162	0.368	25/41	4/9	142/27	2/6
RB373	4/4	0.171	1.034	1.188	1.230	0.658	56/34	7/13	153/11	2/10
RB377	4/4	1.974	1.099	1.060	1.165	−0.224	158/67	4/7	350/22	4/90
RB380	4/4	0.217	1.027	1.178	1.210	0.716	227/48	3/10	324/7	3/3
RB382	4/4	0.644	1.005	1.078	1.082	0.884	271/75	3/90	148/8	0.5/4
RB383	4/4	0.244	1.051	1.192	1.253	0.559	45/64	2/18	153/9	4/10
RB384	4/4	0.707	1.055	1.367	1.441	0.712	11/28	1/6	155/56	1/1
RB489	8/8	0.421	1.037	1.186	1.230	0.654	56/20	4/15	147/4	4/7
RB491	4/4	42.517	1.896	1.152	2.190	−0.654	74/11	2/3	332/47	4/53
RB492	4/4	0.236	1.065	1.034	1.102	−0.307	44/58	1/3	179/24	1/12
RB508	4/4	0.609	1.221	1.068	1.304	−0.502	55/13	1/2	319/24	1/7

Table 1 (*continued*)

SITE	*N*/*n*	K_m (10^{-3})	Mean AMS parameters				Mean eigenvectors			
			L	*F*	*P*	*T*	K_{max}		K_{min}	
							Dec/inc	*z*/*e*	Dec/inc	*z*/*e*
RB520	4/4	8.061	1.130	1.727	1.952	0.639	170/33	4/16	314/51	3/6
RB523	4/4	7.482	1.573	1.646	2.588	0.047	250/5	0/1	159/7	0/1
RB525	4/4	6.888	1.090	1.187	1.296	0.335	323/68	4/22	105/18	3/11
RB526	4/4	0.240	1.018	1.093	1.113	0.664	232/6	5/12	337/69	2/5
RB527	8/8	2.316	1.095	1.066	1.168	−0.203	230/7	6/15	323/24	11/22
RB532	4/4	8.692	1.201	1.073	1.288	−0.443	71/18	2/4	163/5	3/7
Mean		7.535	1.146	1.305	1.526	0.305				

N, number of specimens measured per site; *n*, number of specimens included in the AMS means; K_m, mean magnetic susceptibility (SI units); *L*, magnetic lineation (K_{max}/K_{int}); *F*, magnetic foliation (K_{int}/K_{min}); *P*, degree of anisotropy (K_{max}/K_{min}); *T*, Jelinek's parameters (ln *F* − ln *L*)/(ln *F* + ln *L*); dec, declination; inc, inclination; *z* and *e*, semiangles of the minor and major axes of the 95% confidence ellipse, respectively (modified from Raposo and Egydio-Silva, 2001). Anisotropy of Low-Field Magnetic Susceptibility Data for the different sectors of the Ribeira belt (SE Brazil).

value of ∼1.36, which is high compared with *P* values reported in granitic rocks. The shape parameter *T* varies from −0.19 up to 0.74; oblate ellipsoids ($T>0$) are predominant in the area (16 out of 19 sites) and only three sites display prolate ellipsoids.

The magnetic lineations (K_1) and foliations (planes normal to K_3) determined for the northern domain are relatively scattered (Fig. 7a). However, the magnetic lineation trends mainly ENE–WSW and plunges gently to moderately ENE to ESE. The mean orientation of K_1 is 27–N70°E. The poles to the magnetic foliation are more dispersed, but they define a preferred orientation of the magnetic foliation in the range N10–30°E dipping gently to ESE. The magnetic foliation and lineation map (domain A on Fig. 10) show that the dispersion of the measurements is mainly due to two characteristics of the northern domain: (1) farther north, the trend of the magnetic foliation consistently curves from NNE to NW; the lineation displays a correlated change in direction, and (2) the western and eastern sides of the northern domain show contrasting magnetic fabrics that suggest a variation in strain regime. Westwards, the magnetic foliation dips gently to E or NE and the magnetic lineation is preferentially oriented at high angle to the direction of the magnetic foliation and the pitch of the lineation ranges from 55 to 85° (Fig. 8). This is in good agreement with a dominant thrust tectonic regime, as suggested by kinematic indicators. Eastwards, this fabric is progressively replaced by an eastward steeply dipping foliation bearing a lineation sub-parallel to the strike of the foliation (Figs. 9 and 10). The pitch of the lineation ranges from 0 to ∼45° and suggests a distributed transpressional deformation with dominant transcurrent displacement. This result is in good agreement with the strain repartition in the 2D numerical models shown in Vauchez et al. (1994).

3.3.3. The central domain

Fifteen sites were sampled in the central domain of the belt (Figs. 2 and 3) and AMS individual measurements were performed on 183 cylindrical specimens (Table 1). The magnetic characteristics in this domain are similar to those in the northern and southern domains. The mean magnetic susceptibility K_m varies from ∼0.4 to $\sim 30\times10^{-3}$ SI and K_m is $<1.0\times10^{-3}$ SI for only 4 out of 15 sites (Table 1). The anisotropy degree *P* ranges from ∼1.03 to ∼4.31 with an average value of 1.13. The shape parameter *T* ranges from ∼0.07 to ∼0.83 with an average value of 0.56.

The directions of K_1 and K_3 of the low-field susceptibility ellipsoid for the 15 sites are shown in Figs. 7c and 10. K_1 displays a large variability; it is distributed along a great circle that corresponds to the mean magnetic foliation plane (N54°E–42°SE) (Fig. 7c). A similar dispersion characterizes the orientation of the lineations observed in the field. In contrast, dispersion of magnetic foliations (K_3) is less dispersed (Fig. 3), with a tendency to concentrate close to the pole to the observed foliation (47 to N324°).

4. Discussion

The main objectives of this study were: (1) to compare the magnetic and the tectonic fabrics in high-grade mylonites to validate the use of AMS fabric as a proxy for the structural/kinematic fabric, and (2) to use AMS to map the foliations and lineations in the domain where a transition in deformation mechanism occurs to better constrain how this change is accommodated.

The comparison of the magnetic and tectonic fabrics was mostly performed in the southern domain where mylonites, displaying clear foliations and lineations, are abundant and to a lesser extent in the central domain where mylonitic fabrics are less common. A good agreement is usually observed between the axes of the magnetic and tectonic fabrics observed in the field (compare Figs. 3 and 10). In the southern domain, the stretching lineations are sub-parallel to the foliation plane (transcurrent regime predominant) and the magnetic fabric is usually concordant with the tectonic fabric observed in the field. However, in some places outside the transcurrent shear zones, the magnetic lineation

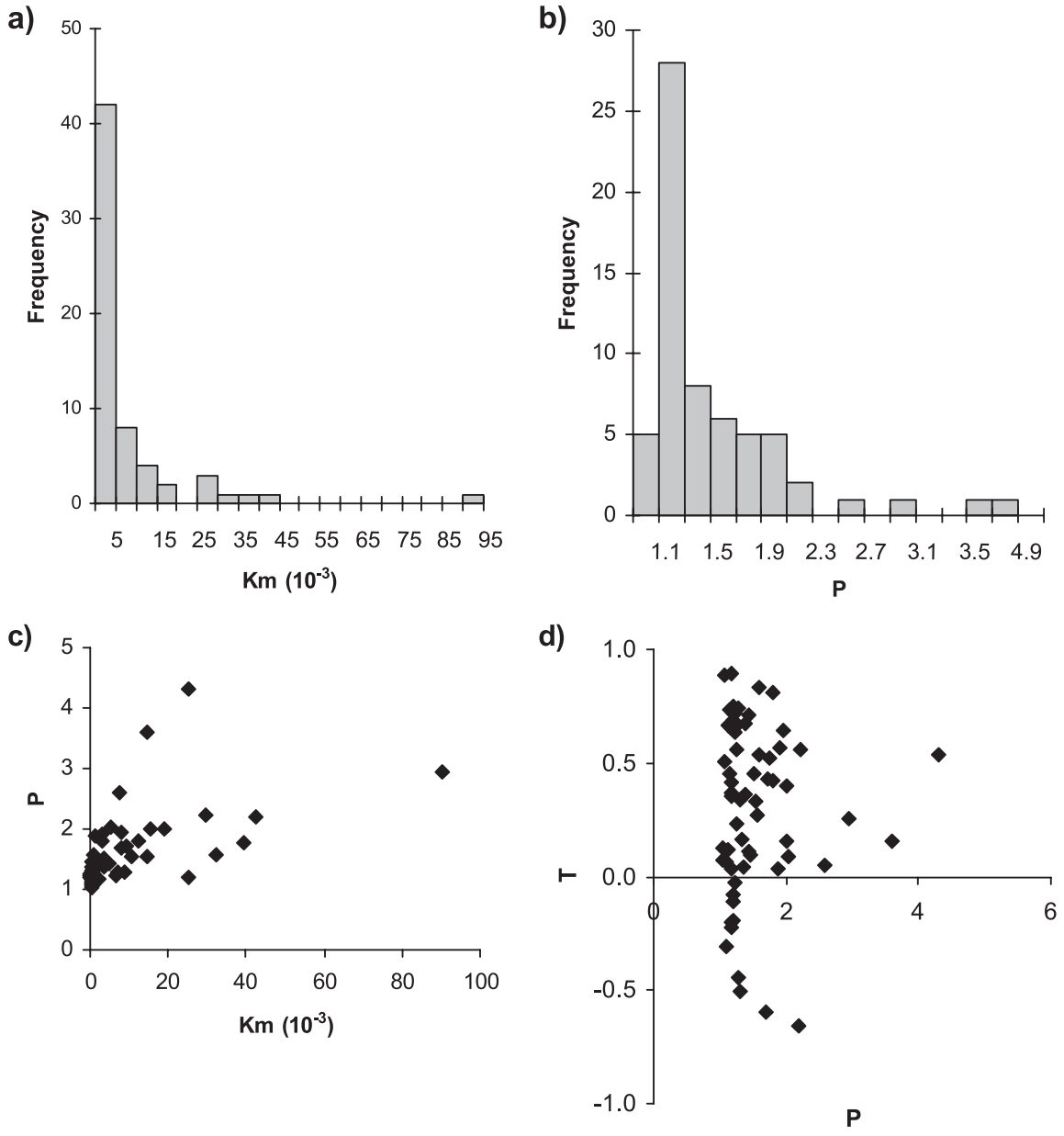

Fig. 6. Anisotropy of magnetic susceptibility (AMS) scalar data (Raposo and Egydio-Silva, 2001). (a) Mean magnetic susceptibility (K_m) frequency histogram. (b) Degree of anisotropy (P) frequency histogram. (c) P versus K_m plot. (d) P versus T (Jelinek's parameter) plot.

is at a high angle to the direction of the magnetic foliation. This belt-normal lineation direction was only rarely observed in the southern domain and is evidence of the compressive component of the transpressional deformation regime.

In the central and northern domains, there is good agreement between the field and magnetic foliations (Figs. 3 and 10). Because of a lack of visible lineations in these rocks, the direct comparison of the magnetic and tectonic lineations is not possible, except in mylonites that outcrop in narrow transcurrent shear zones in the central domain. In this latter case, the correlation is good, as in the transcurrent shear zones of the southern domain. As a whole, comparison of the observed tectonic fabric and the measured magnetic fabric support the use of AMS fabric in granulitic rocks as a proxy for the tectonic fabric, and thus may be reliably used to study complex fabric pattern in transpressional orogens when direct observation is lacking.

The AMS technique allowed us to complete the foliation/lineation map at the regional scale and to better constrain the transition from a transpressional regime with orogen-parallel movement within the southern domain to a thrusting regime within the northern domain, where displacements were dominantly oblique or transverse to the belt. The patterns of magnetic foliation and lineation revealed several new characteristics that shed light on how variation in dominant strain regime was accommodated.

The northern domain (domain A in Fig. 10) displays a

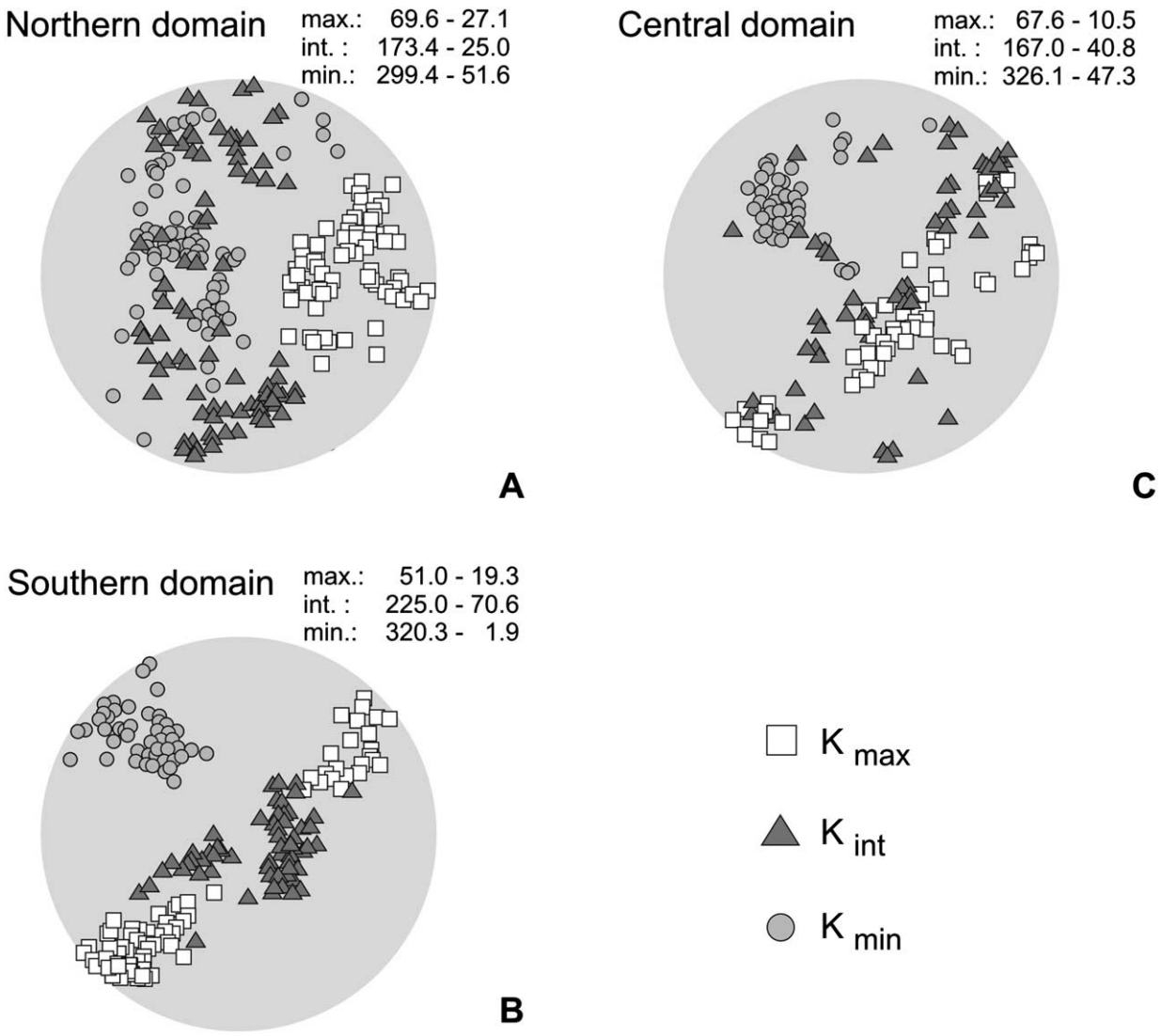

Fig. 7. Magnetic fabrics determined from AMS for the studied region. Plots are lower hemisphere, equal area stereonet.

structural/magnetic fabric more heterogeneous than previously thought. AMS data highlight the existence of two sectors characterized by contrasted magnetic fabric: (a) eastward, steeply dipping magnetic foliations bearing lineations that trend almost parallel to the foliation direction dominate. The magnetic lineation in the foliation plane is, in many cases, significantly different from horizontal (pitch ~30°) suggesting that the vertical component of motion was not negligible even if the main component was along-strike. This pattern is consistent with a transpressional deformation regime and suggests incipient strain partitioning, and (b) westward, the dip of the magnetic foliation decreases and the pitch of the magnetic lineation increases. These variations suggest that the deformation regime is still transpressional since oblique thrusting dominates and the thrust component increases westward.

In the central domain (domain B in Fig. 10) composite magnetic fabrics with both 'strike-slip' and 'thrust' types mark the transition between dominantly transcurrent and dominantly contractional deformations. This complex pattern is correlated in the field with the development of narrow strike-slip shear zones active under granulite-facies conditions. This suggests that strain localization was more efficient in the central domain relative to the northern domain and marks the transition with the southern domain (domain C in Fig. 10) where transcurrent motion is largely localized in the Alem-Paraiba transcurrent shear zone (e.g. Egydio-Silva et al., 2002).

Interestingly, the magnetic fabric at the junction between the southern (C) and central (B) domains highlights the orientation of the Alem-Paraiba shear zone, which follows the Paraiba do Sul River (Fig. 10), oblique relative to the 'strike-slip' type fabric in the central and northern domains. Porcher (1997) has shown that the synkinematic metamorphic conditions in mylonites from the Alem-Paraiba shear zone are slightly lower than in the granulites of the central domain, suggesting diachronous deformation. Altogether, the variations in synkinematic PT conditions

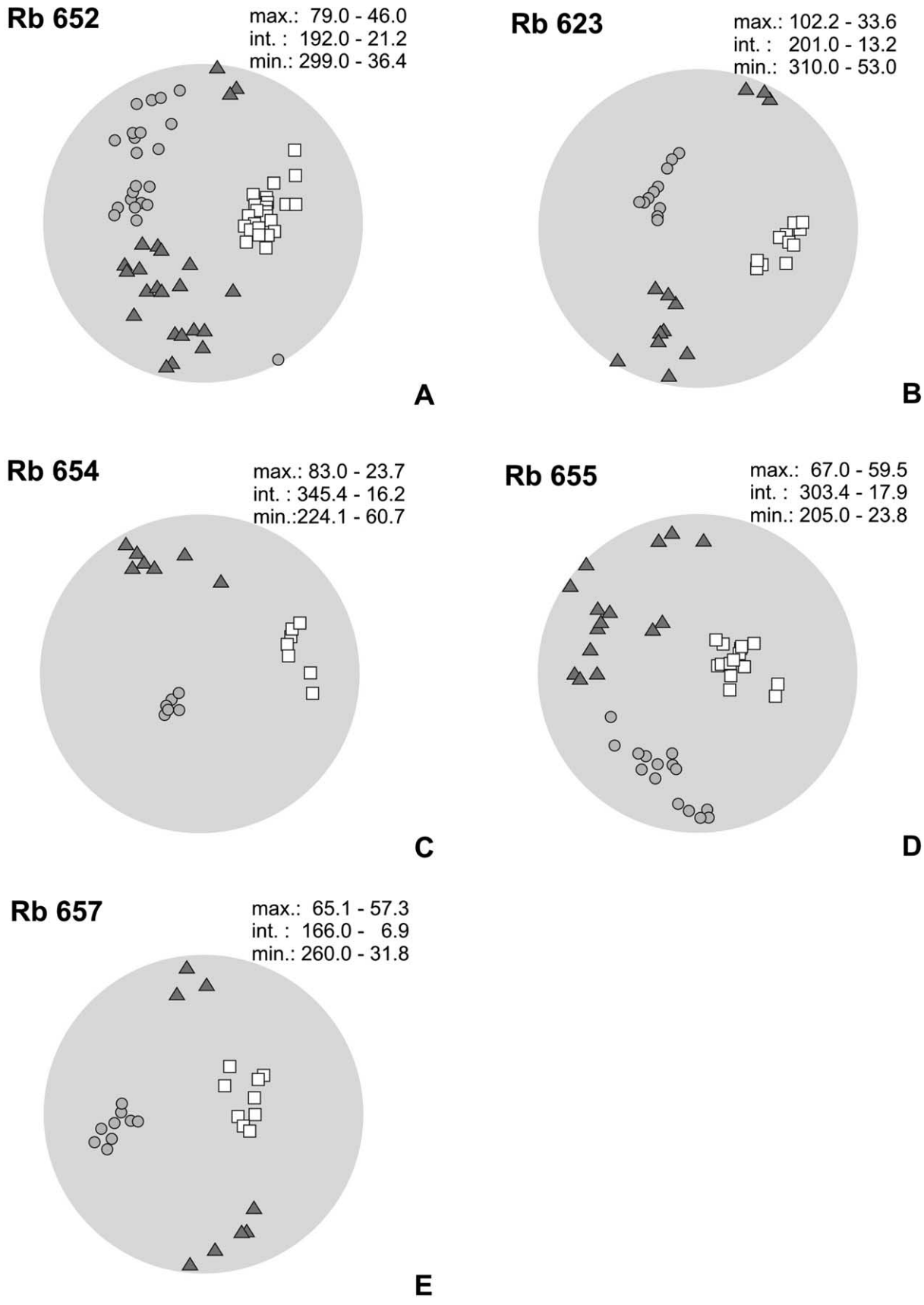

Fig. 8. Magnetic fabrics of the northern domain showing a high angle between magnetic lineations and the magnetic plane directions. A–E are samples from westward subdomain in the northern region of the Ribeira belt.

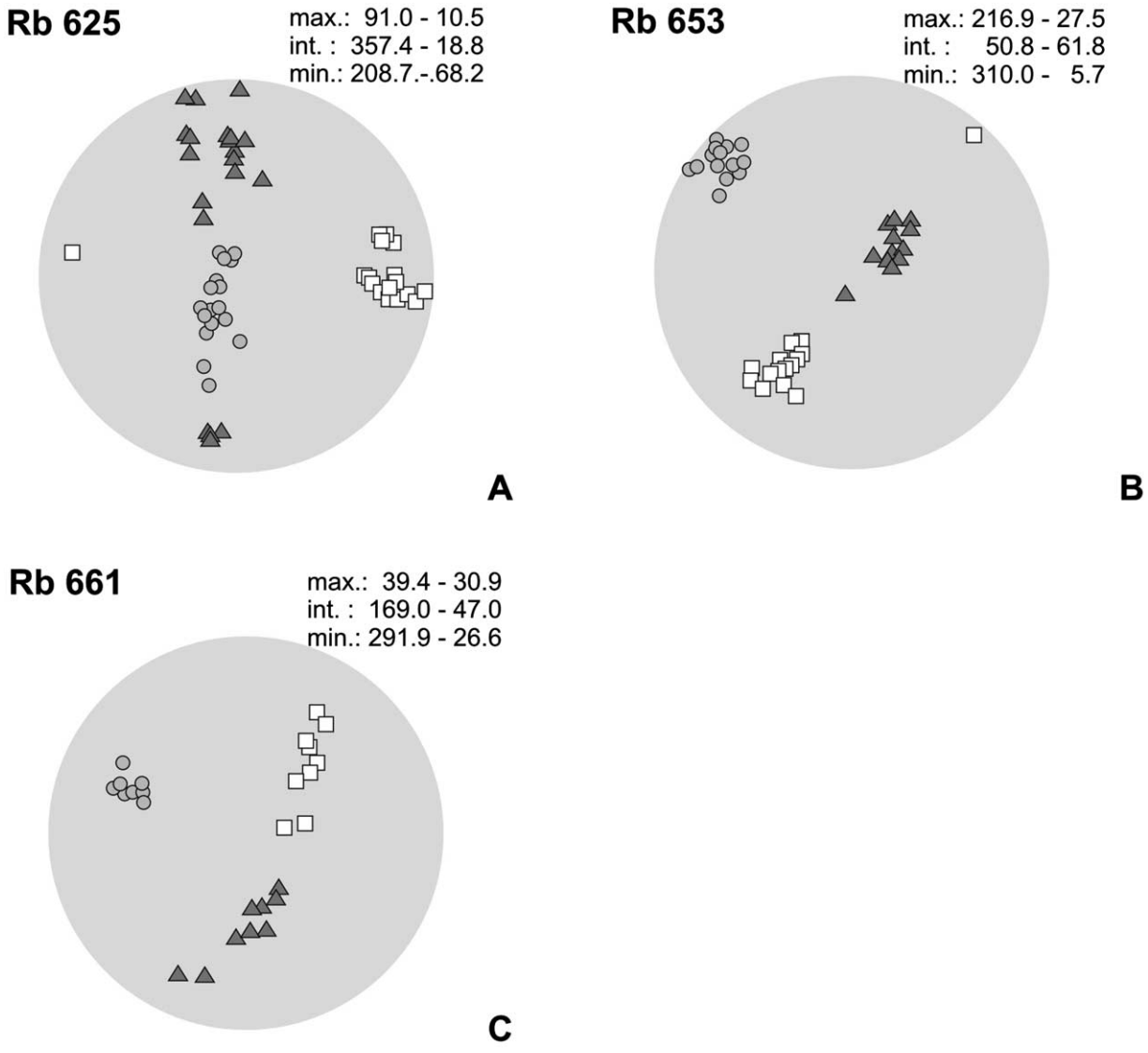

Fig. 9. Examples of magnetic fabrics of the northern domain showing the magnetic lineation directions sub-parallel the magnetic plane directions. A–C are samples from the eastward subdomain in the northern region of the Ribeira belt.

and the structural/magnetic fabric provide support that the Alem-Paraiba shear zone is slightly younger, and thus crosscut the 'strike-slip' fabric of the central domain.

Complex patterns of lineation and foliation are common in transpressional belts and curved shear zones (e.g. Teyssier et al., 1995; Corsini et al., 1996; Lin and Jiang, 2001). For example, the foliations and lineations mapped by Lin and Jiang (2001) in the southern Knee Lake area of the Superior Province of Manitoba, Canada display relationships suggesting variable contributions of strike-slip and thrust-faulting along the narrow southern Knee Lake shear zone. These variations are likely related to bending of the shear zone, which results in variable obliquity between the shear zone and the average relative motion on both sides of the shear zone. The situation is, however, different in the Central Ribeira belt where the entire belt is bent from NS to ENE–WSW. The transition from contraction-dominated to transcurrent-dominated transpression occurs over a segment of orogen >100 km long and ~ 50 km wide. The width of the contraction-dominated domain is progressively reduced southward and the transition from mostly transcurrent to mostly contractional deformation is progressive, with the dip of the foliation and the pitch of the lineation in the foliation varying smoothly (Fig. 11).

Hoffman (1987) shows that an arcuate tectonic system developed along the eastern boundary of the Archean Slave Province, northwestern Canada, linking a contraction-dominated transpressional domain (the Thelon suture–Queen Maud uplift domain) to a transcurrent-dominated transpressional domain (the Great Slave Lake shear zone). The domain where the transition in deformation mechanism occurs accommodates the termination of the Great Slave Lake shear zone, interpreted by Hoffman (1987) as a continental transform fault. There is, however, no detailed

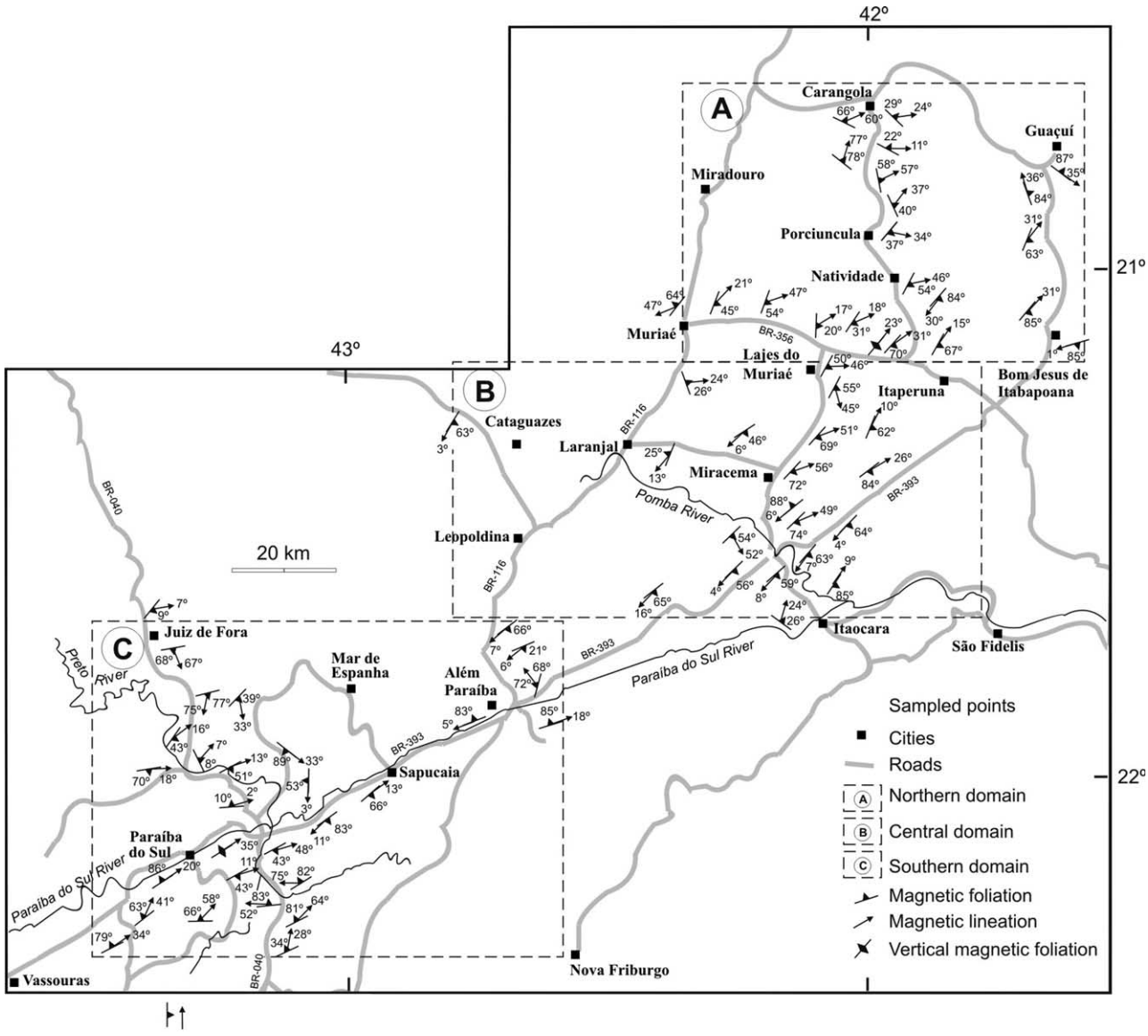

Fig. 10. Map showing the magnetic lineations and foliations in the study area.

data on how the transition from contractional-transpression to transcurrent-transpression is accommodated at the end of the Great Slave Lake shear zone; a model similar to the Central Ribeira belt might apply.

5. Conclusion

As suggested by Bascou et al. (2002) and Borradaile and Gauthier (2003), the comparison of the AMS fabric with the tectonic fabric developed in granulite-facies mylonites supports the use of magnetic fabric as a good proxy of the tectonic fabric in high grade rocks. Thus, this technique is well suited to remedying the scarcity of visible mineral-stretching-lineations inherent to deep crustal levels. Therefore, structural/kinematic analysis may be carried out in the deeply exhumed parts of orogens with increased reliability, resulting in better constrained tectonic models. Moreover, it becomes possible to obtain an improved image of the deformation pattern in areas that have undergone complex deformation regimes (transpressional or transtensional).

In the Ribeira belt, AMS measurements at the transition between the contraction-dominated northern domain and the transcurrent-dominated southern domain provide new insights into how the transition between these two deformation regimes was accommodated in a broad transpressional zone where strike-slip and thrusting coexist at various scales (Fig. 11). This transitional domain is subdivided into two subdomains where either contractional deformation or transcurrent deformation dominates. In each subdomain, however, the deformation regime was transpressional since a non-negligible component of vertical motion was associated with the dominant transcurrent flow in the eastern subdomain and oblique-thrusting is the rule in

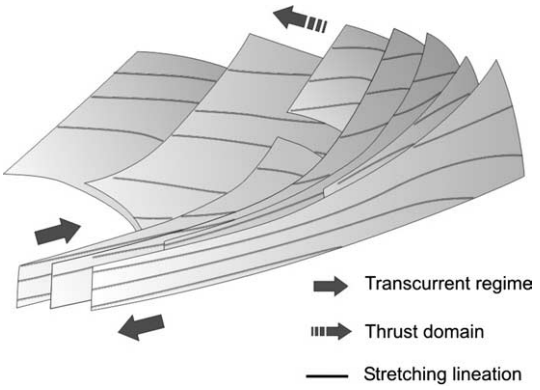

Fig. 11. Diagram illustrating how deformation and kinematics vary along the different domains in the Ribeira belt.

the thrust-dominated western subdomain. Strain partitioning therefore did not occur to a large degree, since the measured fabric is generally consistent with composite deformation regimes. Similarly, the type of fabric remains homogeneous over large areas, suggesting that strain is distributed rather than localized, independent of regime. The absence of efficient strain partitioning and localization are likely due to the high temperature prevailing during deformation that favoured homogeneous deformation.

The AMS data from this area show that while the magnetic foliation poles are well grouped, the magnetic lineations spread out from parallel to normal to the foliation direction. This observation, together with the homogeneity of the metamorphic conditions across the studied area, suggests that both deformation regimes result from a single tectonic evolution rather than from a polyphase deformation. It also points to a limited strain partitioning; the transition is gradational and fabrics suggesting oblique kinematics are more common than purely transcurrent or purely thrust fabrics. This study also suggests that strain localization varies from N to S. In the northern domain, where thrust tectonics dominate, there is little evidence of strain localization, whereas to the south, strain localization in strike-slip shear zones increases significantly with transcurrent deformation outside the shear zones, also indicated by AMS data. This contrast in the effectiveness of strain localization may result either from the accommodation of increasing lateral offset to the south. It is possible that under high temperature conditions to strain localization depends on the dominant deformation regime, leading to a more distributed strain for dominantly contractional tectonics and a more localized deformation for dominantly transcurrent tectonics.

Acknowledgements

This study was supported by international projects (Brazil/France) CAPES/COFECUB (287/99/01-II) and USP/COFECUB (28/96). We are indebted to Frantisek Hrouda, Basil Tikoff and Andrea Tommasi whose comments and suggestions have helped us to substantially improve the manuscript. We also acknowledge Eric Tohver for English improvements.

References

Bascou, J., Raposo, M.I.B., Vauchez, A., Egydio-Silva, M., 2002. Titanohematite LPO and magnetic anisotropies in high-temperature mylonites. Earth and Planetary Science Letters 198, 77–92.

Borradaile, G.J., 1988. Magnetic susceptibility, petrofabrics and strain—a review. Tectonophysics 156, 1–20.

Borradaile, G.J., 1990. Magnetic susceptibility in slates: structural, mineralogical and lithological influences. Tectonophysics 172, 215–222.

Borradaile, G.J., 2001. Magnetic fabrics and petrofabrics; their orientation distributions and anisotropies. Journal of Structural Geology 23, 1581–1596.

Borradaile, G.J., Gauthier, D., 2003. Emplacement of an Archean gneiss dome, northern Ontario, Canada. Inflation inferred from magnetic fabrics. Tectonics 22 (2), 6.1–6.8.

Borradaile, G.J., Henry, B., 1997. Tectonic application of magnetic susceptibility and its anisotropy. Earth Science Reviews 42, 49–93.

Borradaile, G.J., Lagroix, F., 2000. Thermal enhancement of magnetic fabrics in high grade gneisses. Geophysical Research Letters 27, 2413–2416.

Borradaile, G.J., Lagroix, F., 2001. Magnetic fabrics reveal upper mantle flow fabrics in the Troodos ophiolite complex, Cyprus. Journal of Structural Geology 23, 1299–1317.

Bouchez, J.L., 1997. Granite is never isotropic: an introduction to ASM studies of granite rocks. In: Bouchez, J.L., Hutton, D.H.W., Stephens, W.E. (Eds.), Granite: From Segregation of Melt to Emplacement Fabrics. Kluwer Academic Publishers, Dordrecht, pp. 95–112.

Bouchez, J.L., 2000. Anisotropie de susceptibilité magnétique et fabrique des granites. Comptes Rendus de L'Academie de Science 330, 1–14.

Bouchez, J.L., Gleizes, G., Djouadi, T., Rochette, P., 1990. Microstructures and magnetic susceptibility applied to emplacement kinematics of granites: the examples of the Foix pluton (French Pyrenees). Tectonophysics 184, 157–171.

Butler, R.F., 1992. Paleomagnetism: Magnetic Domains to Geologic Terranes. Blackwell Scientific Publications, Boston. 319pp.

Corsini, M., Vauchez, A., Caby, R., 1996. Ductile duplexing at a bend of a continental-scale strike-slip shear zone: example from NE Brazil. Journal of Structural Geology 18 (4), 385–394.

Egydio-Silva, M., Vauchez, A., Bascou, J., Hippertt, J., 2002. High-temperature deformation in the neoproterozoic transpressional Ribeira belt, southeast Brazil. Tectonophysics 352, 203–224.

Ellwood, B.B., 1980. Application of anisotropy of magnetic susceptibility method as an indicator of bottom-water flow direction. Marine Geology 34, M83–M90.

Ellwood, B.B., 1982. Estimates of flow direction for calc-alkaline welded tuffs and paleomagnetic data reliability from anisotropy of magnetic susceptibility measurements; central San Juan Mountains, Southwest Colorado. Earth and Planetary Science Letters 59, 303–314.

Ferré, E., Teyssier, C., Jackson, M., Thill, J.W., Rainey, E.S.G., 2003. Magnetic susceptibility anisotropy: a new petrofabrics tool in migmatites. Journal of Geophysical Research 108 (B2), 2086–2100.

Flood, R.D., Kent, D.V., Shor, A.N., Hall, F.R., 1985. The magnetic fabric of surficial deep-sea sediments in the HEBBLE area (Nova Scotian continental rise). Marine Geology 66, 149–167.

Goldstein, A., Brown, L.L., 1988. Magnetic susceptibility anisotropy of mylonites from Brevard zone, North Caroline, USA. Physics of the Earth and Planetary Interiors 51, 290–300.

Hoffman, P.F., 1987. Continental transform tectonics: Great Slave Lake shear zone (ca. 1.9 Ga), northwest Canada. Geology 15, 785–788.

Hrouda, F., 1982. Magnetic anisotropy of rocks and its application in geology and geophysics. Geophysical Survey 5, 37–82.

Hrouda, F., 1993. Theoretical models of magnetic anisotropy to strain relationship revisited. Physics of the Earth and Planetary Interiors 77, 237–249.

Hunt, C.P., Moskowitz, B.M., Banerjee, S.K., 1995. Magnetic properties of rocks and minerals. In: Ahrens, T.J. (Ed.), Rock Physics and Phase Relations. A Handbook of Physical Constants (3). American Geophysical Union, pp. 189–204.

Jelinek, V., 1977. The statistical theory of measuring anisotropy of magnetic susceptibility of rocks and its application. Geofizika Brno, p. 88.

Knight, M.D., Walker, G.P.L., Ellwood, B.B., Diehl, J.F., 1986. Stratigraphy, paleomagnetism, and magnetic fabric of the Toba Tuffs: constraints on the sources and eruptive styles. Journal of Geophysical Research 91, 10355–10382.

Lin, S., Jiang, D., 2001. Using along-strike variation in strain and kinematics to define the movement direction of curved transpressional shear zones: an example from northwestern Superior Province, Manitoba. Geology 29, 767–770.

Porcher, C., 1997. Relationships between metamorphism and deformation in Ribeira belt: Três Rios and Santo Antônio de Pádua region (RJ), eastern Brazil. PhD Thesis. Rio Grande do Sul Federal University, Brazil.

Raposo, M.I.B., Egydio-Silva, M., 2001. Magnetic fabric studies of high-grade metamorphic rocks from Juiz de Fora Complex, Ribeira belt, southeastern Brazil. International Geology Review 43, 441–456.

Rochette, P., Jackson, M., Aubourg, C., 1992. Rock magnetism and the interpretation of anisotropy of magnetic susceptibility. Review of Geophysics 30, 209–226.

Siegesmund, S., 1996. The significance of rock fabrics for the geological interpretation of geophysical anisotropies. Geotektonik Forschung 85, 1–123.

Sollner, F., Lammerer, B., Weber-Diefenbach, K., 1991. Die krustenent-wicklung in der kustenregion nordlich von Rio de Janeiro/Brasilien. Munchner Geologische Helfe 4, 1–101.

Teyssier, C., Tikoff, B., Markley, M., 1995. Oblique plate motion and continental tectonics. Geology 23, 447–450.

Trompette, R., 1994. Geology of Western Gondwana (2000–500 Ma). A.A. Balkema, Rotterdam. 350pp.

Uhlein, A., Trompette, R., Egydio-Silva, M., 1998. Proterozoic rifting and closure, SE border of the São Francisco craton, Brazil. Journal of South American Earth Sciences 11, 191–203.

Vauchez, A., Tommasi, A., Egydio-Silva, M., 1994. Self-indentation of a heterogeneous continental lithosphere. Geology 22, 967–970.